

# BEAM DYNAMICS ASPECTS FOR THE APT INTEGRATED LINAC\*

S. Nath, K. R. Crandall<sup>†</sup>, E. R. Gray, T. P. Wangler and L. M. Young  
Los Alamos National Laboratory, Los Alamos, NM 87545

## Abstract

The accelerator-based production of tritium calls for a high-power cw proton linac. The current Los Alamos design uses an integrated approach in terms of accelerating structure. The front part of the accelerator uses normal-conducting (NC) structures while most (>80%) of the linac structure is superconducting (SC). Here, we report the beam-dynamics rationale used in the integrated design and present particle simulation results.

## INTRODUCTION

The linac for the production of tritium calls for 100 mA of cw proton beam to be delivered onto a production target. Previous design [1] consisted entirely of normal-conducting structures. In that design, we minimized the number of transitions between accelerating structures. In addition, the phase advances per unit length in both the transverse and longitudinal motion were tailored to be continuous at the only transition point i.e. RFQ and the CCDTL at 6.7 MeV. The structure beyond 100 MeV was also a NC coupled-cavity structure.

At higher energies, however, there are some advantages of using SC rf-cavity structures discussed in detail elsewhere [2,3]. In brief, it allows comparatively larger bore size minimizing the risk of beam loss - an issue of utmost importance for such a high power linac. Considerably more operational flexibility is another advantage of using SC structures at higher energies. A substantially higher power efficiency is obviously the major attraction in terms of life-time operational cost. To arrive at an optimum integrated design, we studied several design-schemes in terms of lattice, focusing strength and number of accelerating cavities per cryomodule in the SC section. The design features of the linacs are described in an accompanying paper [3]. In the following sections, we describe the beam dynamics and simulated performances of a few of the design-options studied so far.

## DESIGN OVERVIEW

At present, 217 MeV, which corresponds to the end of a supermodule in the NC section is chosen as the transition energy between the NC low-energy (LE) linac to the SC high-energy (HE) linac. It is a good compromise in terms of the desire to switch at the lowest possible energy to maximize the benefits of the SC linac, and confidence in the SC-cavity performance for the shortened elliptical cavity which increases with the design velocity.

Beyond 217 MeV, the SC structures accelerate the beam to a nominal energy of 1.7 GeV. The HE SC linac is comprised of two sections, a medium- $\beta$  section with identical cavities optimized for a velocity  $\beta=0.64$ , and a

high-beta section with identical cavities optimized for a velocity  $\beta=0.82$ . Each section consists of a sequence of identical cryostats. The rationale for the two-velocity section/5-cell-cavity architecture is based on the velocity-acceptance characteristics of the cavities as a function of the number of cells per cavity. Detailed analysis is contained in Ref. 2.

Two design scenarios for the SC linac section are considered. One uses SC quadrupole magnets laid out in a FODO lattice. The magnets are contained within the cryostats alternating with the cavities. In another option, the quadrupole magnets are laid out in a doublet (FDO) lattice outside the cryomodules. Heretofore, we refer them to as singlet and doublet design respectively.

## SINGLET DESIGN

In the singlet design, there are three Nb cavities in the  $\beta=0.64$  section, while the  $\beta=0.82$  section contains four cavities per cryomodule. The medium- $\beta$  section accelerates the beam through a nominal energy range from 217 MeV to 469 MeV with an average or real-estate accelerating gradient ranging from 1.43 to 1.51 MV/m. The high- $\beta$  section ranges from 469 MeV to 1700 MeV with an average accelerating gradient of 1.89 MV/m. The beam dynamics parameters are listed in Table 1. The length of the focusing period in the transition from the normal to the SC section approximately doubles from 2.0 m to about 3.4 m.

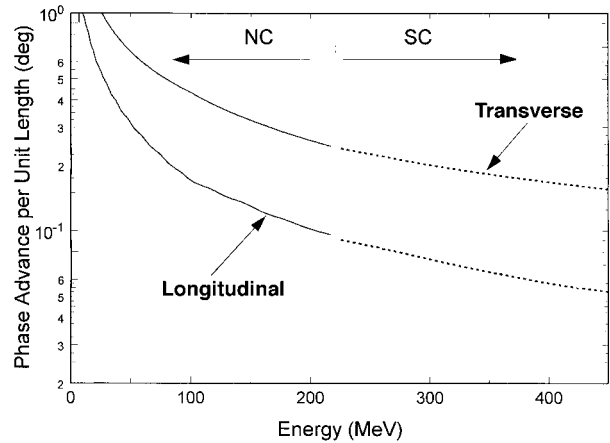


Figure 1. Zero-current transverse and longitudinal phase advance per unit length (degree/cm) across the transition between the NC and SC linac at 217 MeV.

No separate matching section is used to match the beam across the NC/SC transition. Instead, matching is achieved by smoothly ramping the quadrupole strengths, beginning at 24 MeV, so that the focusing strength across the transition is smooth. From 24 MeV to 100 MeV, the gradient is scaled down as  $1/\beta^{0.25}$ . The strength is scaled

\* Work supported by the US Department of Energy  
<sup>†</sup> Amparo Corporation, Santa Fe, NM 87540

as  $1/\beta^{0.40}$  from 100 to 155 MeV, and as  $1/\beta^{0.48}$  from 155 to 217 MeV. This prescription results in a continuous zero-current phase advance per unit length as shown in Figure 1. The average (i.e. real-estate) accelerating gradients across the transition are almost equal as are the average design phases. This makes the zero-current longitudinal phase advance per unit length also continuous across the NC/SC transition point.

**Table 1. Beam Dynamics Parameters for the Singlet SC linac without equipartitioning**

Parameter	Medium- $\beta$ Section	High- $\beta$ Section
Quadrupole lattice type	FODO	FODO
Lattice half period	1.70	2.03
Synchronous phase (deg)	-25 to -35	-30
$\sigma_{t0}$ = Trans. phase adv. per period (zero current)	80 to 52	57 to 25
$\sigma_t$ = Trans. phase adv. per period (space charge)	42 to 25.4	28.3 to 14.4
$\sigma_{l0}$ = Long. phase adv. per period (zero current)	26 to 14.5	25 to 7.5
$\sigma_l$ = Long. phase adv. per period (space charge)	9.1 to 5.8	4.5 to 0.7
$\sigma_t / \sigma_{t0}$	0.5	0.5 to 0.6
$\sigma_l / \sigma_{l0}$	0.3 to 0.2	0.2 to 0.1
Trans. Emit. ( $\pi$ -cm-mrad)	0.0163 to 0.0166	0.0166 to 0.0164
Long. Emit. ( $\pi$ -cm-mrad)	0.045 to 0.046	0.046 to 0.050
Ratio of aperture radius to matched rms beam radius	39 to 43	54 to 70

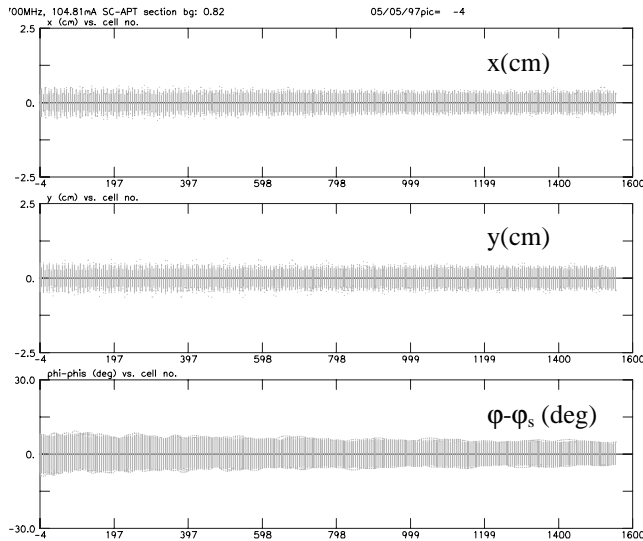


Figure 2.. Transverse and longitudinal profile plots in the “singlet” SC linac from 469 MeV to 1.7 GeV for non-equipartitioned mode of operation.

In the context of the optimization process for the singlet-lattice design, the quadrupole gradient profiles

along the linac must be chosen. As one possibility, merits of equipartitioning [4, 5] were investigated. Detailed results are described in an accompanying paper [6]. Figure 1 and Table 1 correspond to a non-equipartitioned case. For the equipartitioned case, we have a similar, smooth transition as is shown in Ref. 6. The ratio  $\sigma_{0l}/\sigma_{0t}$  decreases from 0.55 at 25 MeV to 0.30 at 1.7 GeV. In the equipartitioned linac, on the other hand, the ratio is nearly constant throughout the linac. It should be noted that equipartitioning requires operating the linac with reduced transverse focusing strength above 25 MeV. The quadrupole strength at the end of the equipartitioned linac is about 55% of the strength in the non-equipartitioned linac.

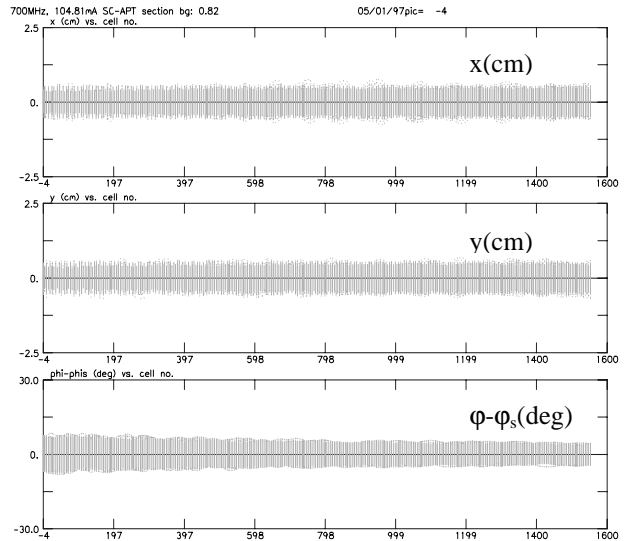


Figure 3. Transverse and longitudinal profile plots in the “singlet” super-conducting linac from 469 MeV to 1.7 GeV for equipartitioned mode of operation.

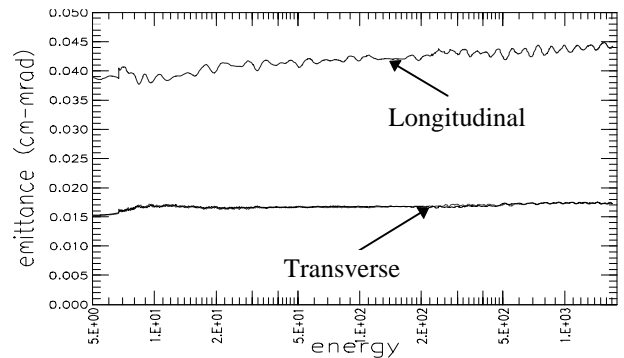


Figure 4. Longitudinal and transverse rms normalized emittance vs. energy for full current in the “singlet” SC linac for equipartitioned mode of operation.

Simulation results without any errors for both the equipartitioned and un-equipartitioned mode are shown in Figures 2 through 4. Initial beam distribution of 100,000 particles originating at the plasma surface of the ion source are followed [7] through the entire linac. Beam-profile plots for full current from 469 MeV to 1.7 GeV in the un-equipartitioned and equipartitioned cases are shown in Figures 2 and 3 respectively. Relative to the rms size, the beam is smaller in the equipartitioned case but in

absolute terms, the beam-size is roughly 55% larger. No oscillations in the profiles indicate a good match in the transition region. Longitudinal and transverse emittance as a function of energy for the equipartitioned case are plotted in Fig. 4. The optimum choice for the quadrupole gradient profile in the final design will also depend on the results of the linac performance, when errors are included.

## DOUBLET DESIGN

In the doublet design for the SC section, the cryomodules contain only the Nb cavities; the room-temperature quadrupoles are placed outside. For the  $\beta=0.64$  section, there are two cavities per period. In the  $\beta=0.82$  section, two configurations were studied; one with two cavities per period and the other with four cavities per period.

In order to achieve a current independent matching between the normal-conducting and SC structure, the quad strengths in the NC section need to be ramped down more than was done in the singlet design. The period-length at 217 MeV for the NC and the SC structures are about 2.0 m and 4.9 m respectively. In order to achieve the same phase advance per unit length at the transition, we start tapering down the field gradient of the quadrupoles in the NC section starting at 100 MeV where  $\sigma_{0i}=77.2^\circ$ . Quadrupole gradients are ramped down to make  $\sigma_{0i}=32.7^\circ$  at 217 MeV reducing the phase advance by equal amounts per period. In the longitudinal plane,  $\sigma_{0l}$  per unit length are the same at the transition for  $\phi_s=-30^\circ$ .

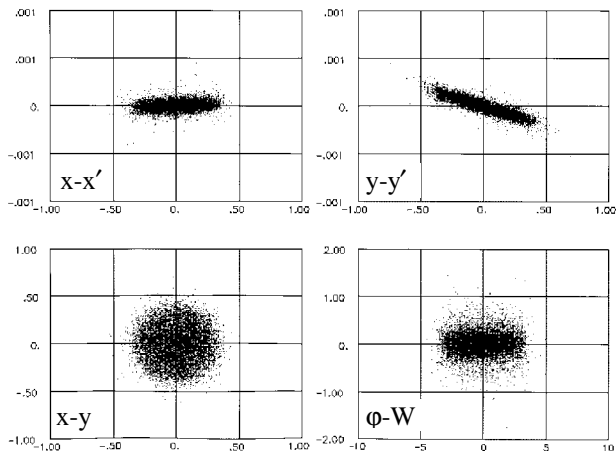


Figure 5. Output phase-space distributions at 1.7 GeV for the doublet design with four cavities per period in the  $\beta=0.82$  section.

The matching between the  $\beta=0.64$  and  $\beta=0.82$  SC-sections starts with finding suitable design phases for the last period of the  $\beta=0.64$  section and the first period of the  $\beta=0.82$  section. The phases in the  $\beta=0.64$  section are then ramped appropriately to achieve a smooth longitudinal transition. For the design with two cavities per period in the  $\beta=0.82$  section, the quads in the  $\beta=0.64$  section need to be ramped up from 5.75 to a final value of 7.75 T/m to match the  $\sigma_{0i}=80^\circ$  value in the first period of the  $\beta=0.82$  section. For the design with four cavities per period, period-lengths are longer. Here, in addition to ramping the quadrupole gradients in the  $\beta=0.64$  section, the gradients in the interface need to be adjusted slightly.

Good matching is achieved for all currents between zero and 100 mA in both the designs described above. It should be emphasized that no special difficulties were encountered in achieving a current independent singlet to doublet match at 217 MeV. The output phase space distributions at 1.7 GeV for the design with four cavities per period in the  $\beta=0.82$  section are shown in Figure 5. The output phase space distributions for the design with two cavities per period look very similar except that it has slightly smaller transverse rms dimension. In both the designs, there is very small growth in the transverse emittance. Figure 6 shows the relationship between maximum rms -beam-size, aperture-size, and maximum transverse coordinate of a particle as a function of energy.

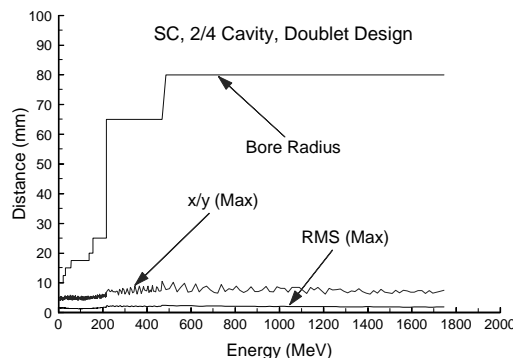


Figure 6. Maximum rms beam-size, aperture size and maximum transverse coordinate of the outermost particle vs. energy.

## CONCLUSION

Beam-dynamics simulations show that both singlet and doublet designs are viable options for the SC linac section. An integrated NC/SC design using either of the options provides the beam quality required for the APT.

## REFERENCES

- [1] S. Nath et al., "Physics Design of APT Linac with Normal Conducting RF Cavities," Proceedings of the 1996 Linear Accelerator Conference, Geneva, Switzerland, August 26-30, 1996.
- [2] Los Alamos National Laboratory APT Conceptual Design Report, LA-UR-97-1329, April 1997.
- [3] G. P. Lawrence and T. P. Wangler, "Integrated Normal-conducting/Superconducting High Power Proton Linac for APT," this conference.
- [4] R. A. Jameson, "On Scaling and Optimization of High Intensity Low-Beam-Loss RF Linacs for Neutron Source Drivers," AIP Conference Proceeding 279, ISBN 1-56396-191-1.
- [5] M. Reiser, "Theory and Design of Charged Particle Beams," John Wiley & Sons, Inc., p573 (1994).
- [6] L. M. Young, "Equipartitioning in a High Current Proton Linac," this conference.
- [7] L. M. Young, "Simulations of the LEDA LEBT with  $H^+$ ,  $H_2^+$ , and  $e^-$  particles," this conference.